View metadata, citation and similar papers at core.ac.uk
brought to you by CORE
provided by Warwick Research Archives Portal Repository

WARWICK
THE UNIVERSITY OF WARWICK

Original citation:
Guo, Z., Tian, Yanling, Liu, Xianping, Wang, F., Zhou, C. and Zhang, D. (2017) Experimental investigation of the tip based micro/nano machining. Applied Surface Science, 426. pp. 406-417.
Permanent WRAP URL:
http://wrap.warwick.ac.uk/94041

Copyright and reuse:
The Warwick Research Archive Portal (WRAP) makes this work by researchers of the University of Warwick available open access under the following conditions. Copyright © and all moral rights to the version of the paper presented here belong to the individual author(s) and/or other copyright owners. To the extent reasonable and practicable the material made available in WRAP has been checked for eligibility before being made available.

Copies of full items can be used for personal research or study, educational, or not-for-profit purposes without prior permission or charge. Provided that the authors, title and full bibliographic details are credited, a hyperlink and/or URL is given for the original metadata page and the content is not changed in any way.

Publisher's statement:
© 2017, Elsevier. Licensed under the Creative Commons Attribution-NonCommercial-NoDerivatives 4.0 International http://creativecommons.org/licenses/by-nc-nd/4.0/

A note on versions:
The version presented here may differ from the published version or, version of record, if you wish to cite this item you are advised to consult the publisher's version. Please see the 'permanent WRAP URL' above for details on accessing the published version and note that access may require a subscription.

For more information, please contact the WRAP Team at: wrap@warwick.ac.uk

warwick.ac.uk/lib-publications

Experimental investigation of the tip based micro/nano machining

Z. Guo[1], Y. Tian*[1,2], X. Liu[2], F. Wang[1], C. Zhou[1], D. Zhang[1]

[1]Key Laboratory of Mechanism Theory and Equipment Design of Ministry of Education, Tianjin University, Tianjin 300072, China

[2]School of Engineering, University of Warwick, Coventry CV4 7AL, UK

Abstract

Based on the self-developed three dimensional micro/nano machining system, the effects of machining parameters and sample material on micro/nano machining are investigated. The micro/nano machining system is mainly composed of the probe system and micro/nano positioning stage. The former is applied to control the normal load and the latter is utilized to realize high precision motion in the *xy* plane. A sample examination method is firstly introduced to estimate whether the sample is placed horizontally. The machining parameters include scratching direction, speed, cycles, normal load and feed. According to the experimental results, the scratching depth is significantly affected by the normal load in all four defined scratching directions but is rarely influenced by the scratching speed. The increase of scratching cycle number can increase the scratching depth as well as smooth the groove wall. In addition, the scratching tests of silicon and copper attest that the harder material is easier to be removed. In the scratching with different feed amount, the machining results indicate that the machined depth increases as the feed reduces. Further, a cubic polynomial is used to fit the experimental results to predict the scratching depth. With the selected machining parameters of scratching direction d3/d4, scratching speed 5μm/s and feed 0.06μm, some more micro structures including stair, sinusoidal groove, Chinese character ‘田’, ‘TJU’ and Chinese panda have been fabricated on the silicon substrate.

Keywords: micro/nano machining; machining parameters; scratching depth

1. Introduction

Nowadays, the fabrication of nanochannel and nanostructure is a hot issue in micro/nano field. There are many different methods, such as photolithography [1], LIGA [2], FIB (Focused Ion Beam) technology [3], nanoimprint [4] and tip based nanomanufacturing (TBN) [5]. Among all of these methods, every technique has its own advantages and special applications, but the tip based micro/nano machining is attracting more and more attention for the low-cost, simple operation and high accuracy. The scanning tunneling microscopy (STM), atomic force microscope

(AFM) and nanoindenter are three common devices for the TBN technology, especially the application of AFM makes this technology greatly developed, and it has successfully combined the chemical and thermal effects to the traditional mechanical removal [6].

In the AFM tip based mechanical nanomanufacturing, the effects of machining parameters including applied normal load, scratching direction, scratching cycles, scratching speed and scratching feed on the machined depth and surface roughness have been investigated by many scholars in the last decades [7-13]. Recently, some researchers focus on the theoretical modeling of scratching depth. Wang studied the relationship between the initial and final nanochannel depth through both theoretically and experimentally [14, 15]. Geng modeled the scratching depth theoretically in both single and multiple scratching, and micro/nano structures were manufactured based on the proposed model [16]. Lin estimated the cutting depth based on regression equations of nanoscale contact pressure factor and specific down force energy, respectively [17].

The probe cantilever of the AFM is essentially a single flexible beam, as a result, the stiffness of the AFM cantilever in the longitudinal direction is different from that in the transverse direction, which affects the experimental results when scratching in different directions. Unfortunately, the tip-sample interface is also affected by the scratching direction due to the tip geometrical asymmetry. These factors make the investigation of scratching direction complex. Moreover, the AFM cantilever is usually very soft in the vertical direction, which makes it sensitive to the environmental changes. Finally, the low positioning precision of the AFM motion platform reduces the machining accuracy in *xy* plane. In order to overcome these shortcomings of the AFM, many different mechanical designs have been proposed for the micro/nano machining. Lee adopted a strain gauge measured load beam to substitute the AFM cantilever [18]. Park designed a displacement-force device to realize the micro/nano machining [19]. Jeong presented an air lubricated hydrostatic sliding mechanism based portable nano probe system [20]. Gozen constructed a nano milling system to fabricate the micro channel [21]. All these designs can realize the micro/nano structure scratching, but they also have obvious drawbacks, such as the overlarge normal load in Lee’s mechanism, the residual friction of the probe shaft in Jeong’s design, and the limitation of machining width in Gozen’s system. As to the position precision in *xy* plane, the piezo-actuated flexure-mechanism is a good choice to solve this problem, which has been studied by many scholars [22-25].

In this paper, a self-developed three dimensional micro/nano machining system is used for the experimental investigation, which mainly includes the probe system and precise positioning stage. The cross-shaped probe suspension mechanism in the probe system effectively avoids the singal axis and low stiffness of the AFM cantilever. Before the scratching experiments, an

examination method is presented to examine the horizontal place of the sample. Subsequently, the scratching parameters including scratching direction, normal load, scratching cycles, scratching speed and scratching feed are systematically investigated and analyzed. Further, the copper sample is scratched and the material removal results are compared with those of silicon samples. Finally, some more micro structures are fabricated on the silicon base with the selected scratching parameters.

2. The micro/nano machining system

All of experiments are performed in a self-developed three dimensional micro/nano machining system, which is shown in Fig. 1. The overall frame applies the gantry structure. Three manual coarse mobile platforms (WN115TM50M, winner optical instruments, China) arranged orthogonally are used to realize the broad adjustment with the full stroke of 50mm and minimal regulating amount of 2 μm. The probe system and the 3-DOF micro/nano positioning stage are the two core parts of the machining system, where, the probe system is used to control the normal force, and the micro/nano positioning stage is used to realize the precise motion in the *xy* plane. The whole system is mounted on a Newport RS-4000 optical table.

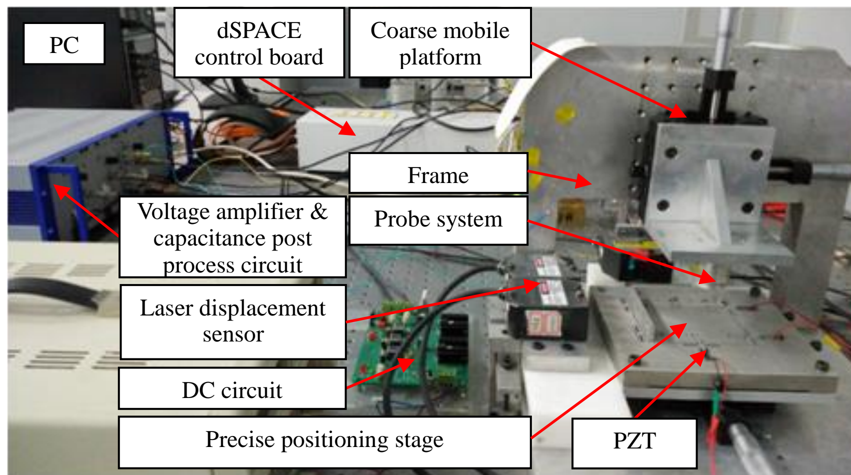

Fig. 1 The three dimensional micro/nano machining system

2.1 The probe system

As shown in Fig. 2(a), the probe system mainly includes the coil, permanent magnetic, cross shaped probe suspension mechanism, diamond probe and aluminum film. The coil and permanent magnetic form the electromagnetic device to provide normal force on the probe, the convert rate from current to electromagnetic force is 78.4μN/mA. The probe suspension mechanism is cross shaped beams, which has better isotropic stiffness in the *xy* plane compared with the AFM

cantilever. Each beam of the probe suspension mechanism organizes the capacitor plates with the aluminum film as well as supports the diamond probe, the constructed four group capacitors are marked as 1-4 in Fig. 3(a), and each group can be used for the scratching depth measurement. Further information about the probe system can reference our previous work [26].

As the machining tool, the Berkovich probe is attached on the bottom of the cross-shaped probe suspension. Due to the three side pyramidal geometry of the probe tip, four perpendicular scratching directions are defined to investigate the effects of scratching direction on the scratching process. The four directions d1-d4 are shown in Fig. 3(b), d1 is the edge forward direction, d2 is the face forward direction, d3 and d4 are the side face forward direction. Each scratching direction is along one beam of the probe suspension mechanism. Thus, the probe must be carefully assembled to ensure the correct position between the probe and the probe suspension mechanism. The horizontal projected area of the tip-sample interface in each scratching direction is also shown in Fig. 3(b), indicating two pyramidal faces of the probe tip contact with the sample in the d1, d3 and d4 direction, and one pyramidal face in the d2 direction.

Related to the probe system, a home-made directive current (DC) circuit is used to drive the coil, which receives the command signals from the I/O interface of a dSPACE DS1103 R&D control board. The capacitance of the formed capacitor is converted to voltage by a post-process circuit (E-509.C3A, PI, Germany) for the further data processing.

2.2 The micor/nano positioning stage

Fig. 2(b) shows a piezoelectric actuator (AE 0505D18F, THORlabs Company, USA) driven 3-DOF micro/nano positioning stage. Six Double Circular Hinge Linkages (DCHL) are used to translate the driving force and decouple the motion, as well as to support the moving platform. The Dual Leaf Parallelogram Hinge (DLPH), as shown in Fig. 1(c), is utilized to guide the motion of the piezoelectric actuator, and further the half cylinder structure is added between the piezoelectric actuator and the DLPH to eliminate the bending moment acting on the piezoelectric actuator. Three laser displacement sensors (LK-H050, Keyence, Japan) provide real time displacement sensing and measurement for the moving platform. The stroke of the stage is beyond 10μm in both x and y direction, and with a positioning precision 37nm in the x direction and 24nm in the y direction. The detailed design process of the stage can be found in reference [27].

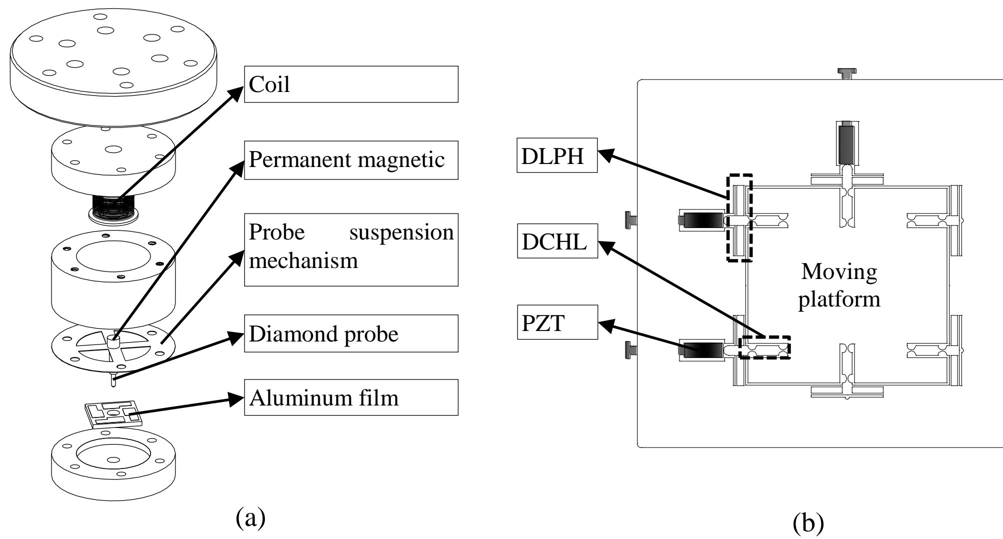

Fig. 2 (a) The exploded review of the probe system; (b) The 3-DOF micro/nano positioning stage

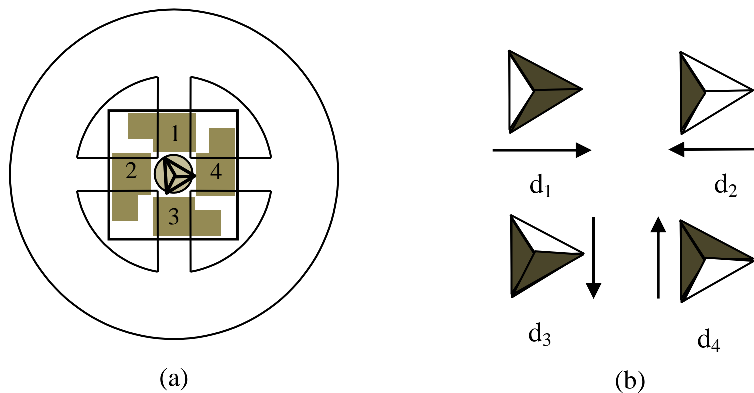

Fig. 3 (a) the probe suspension mechanism and the formed capacitor; (b) defined scratching direction and the horizontal projected area of the tip-sample interface.

3. The experimental investigation

In the experimental investigation, the silicon is firstly selected as the sample for the wide application in semiconductor industry. After micro/nano machining, the sample is cleaned using ultrasonic wash with acetone solution for ten minutes to remove the generated chips, and then the machined micro/nano grooves or structures are measured using AFM (CSPM5500, Benyuan, China).

3.1 The horizontal examination of the sample

In the developed micro/nano machining system, considering the simple operation, the open loop control method is adopted to control the electromagnetic force. As a result, for a constant

normal force, the scratching depth will be affected if the sample is not placed horizontally. Thus, a method to examine whether the sample is placed horizontally is firstly introduced.

A square groove is scratched on silicon base with each groove parallel to one above defined scratching direction, and a group of capacitor is used to measure the scratching depth simultaneously. A linear current is inputted into the probe system to generate electromagnetic force and further drive the probe move in the *z* direction. As shown in Fig. 4, before the contact of the probe tip and sample surface, the displacement is linear to the input current, in this period, the electromagnetic force is completely balanced by the deformation of probe suspension mechanism. As shown in Fig. 4(c), when the probe tip contacts with the sample, the measured displacement appears an inflection point due to the resistance of the sample base. Then the probe is indented into the sample. In the phase of probe indentation, the deformation force of the probe suspension could be neglected for the small indentation depth, so the normal force used for the scratching is approximately the increased electromagnetic force. After that, the electromagnetic force is kept constant and the micro/nano positioning stage is actuated to complete the square motion, simultaneously, the measured displacement of the probe suspension is shown in Fig. 4(d), the constant displacement in every direction means the sample surface is positioned horizontally.

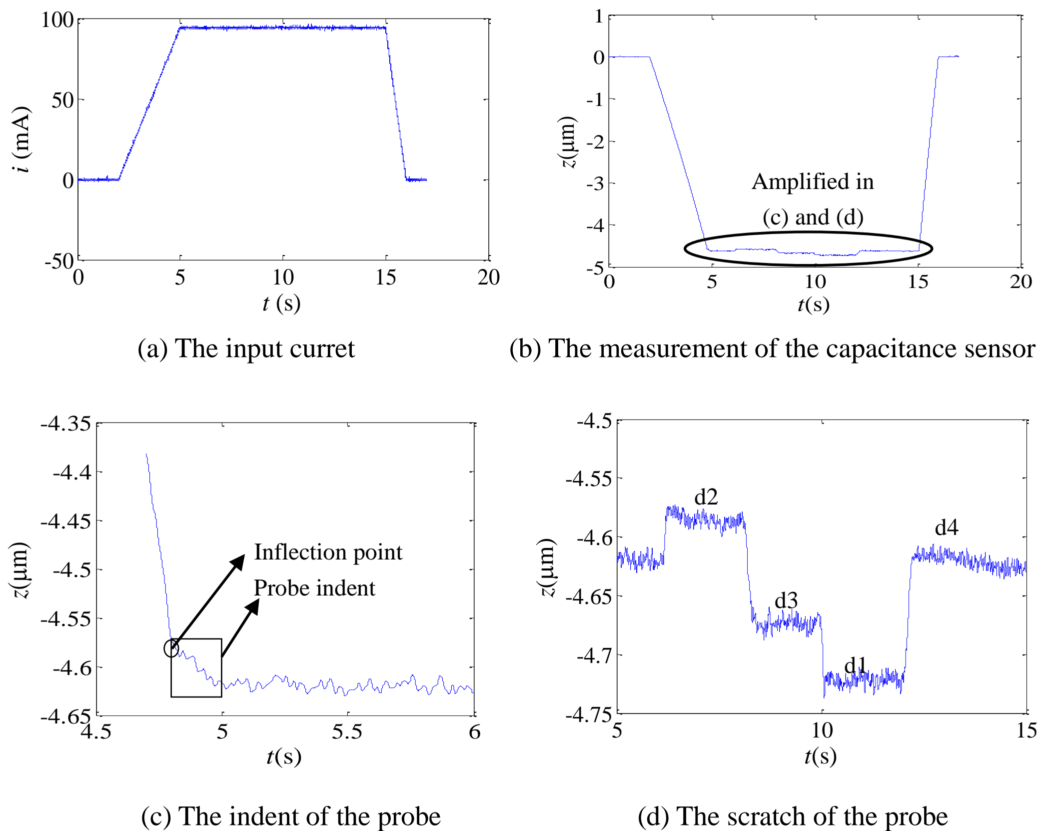

Fig. 4 The horizontal examination of the sample

Ideally, the measured displacement should be constant in all scratching direction, but there are abrupt changes in the direction convert, it can be explained as follows. The capacitor 2 (shown in Fig. 3) is selected to measure the probe displacement, so the applied suspension mechanism beam is along the scratching directions d1 and d2. According to the beam stiffness theory, it is easier to generate deformation in the axial direction than the vertical direction, thus, the beam bends easier in the d1 and d2 directions but with opposite deformation as shown in Fig. 5(b), while it keeps almost undeformed in the d3 and d4 directions as shown in Fig. 5(c). As a result, the beam deforms suddenly when the scratching direction changes. The residual difference of the measured displacement in the d3 and d4 directions may be caused by the assembly error of the probe.

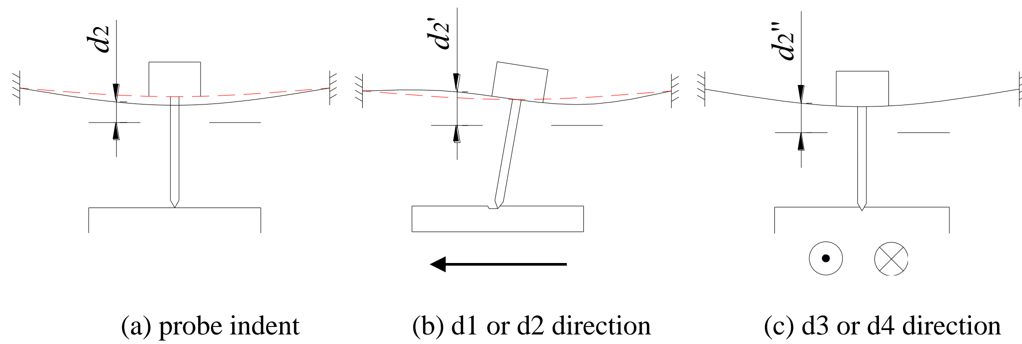

(a) probe indent (b) d1 or d2 direction (c) d3 or d4 direction

Fig. 5 Probe indent and scratching in different direction

3.2 The indentation test

The indentation tests with three different normal loads are firstly implemented on the silicon substrate. Fig. 6(a) and (b) show the relationship of electromagnetic force - measured displacement and load - indentation depth, respectively. In Fig. 6(a), the relationship curve during the probe lift appears inflection in all three indentation tests, which means the probe tip separates from the sample, and then the electromagnetic force is balanced by the deformation of probe suspension mechanism, indicating the electromagnetic force is linear to the measured displacement. Remove the deformation force of the suspension mechanism, the relationship of load – indentation depth is obtained as shown in Fig. 6(b). Where, the normal load is the difference between the electromagnetic force and the deformation force of suspension mechanism, as Eq. (1). It is obvious that after the normal load is reduced to zero, the sample generates plastic deformation with certain indentation depth.

$$F_{\text{normal}} = F_{\text{elec}} - F_{sus} \tag{1}$$

where, F_{normal} is the normal load acted on the sample, F_{elec} is the generated electromagnetic force, F_{sus} is the deformation force of the probe suspension mechanism.

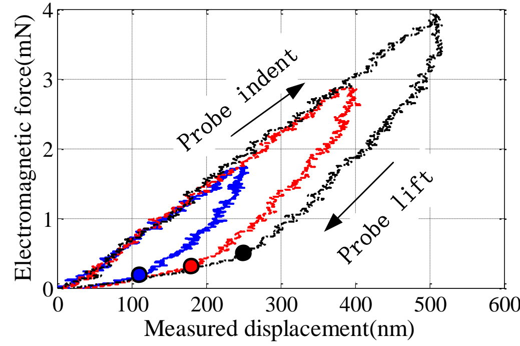

(a) The electromagnetic force versus the measured displacement

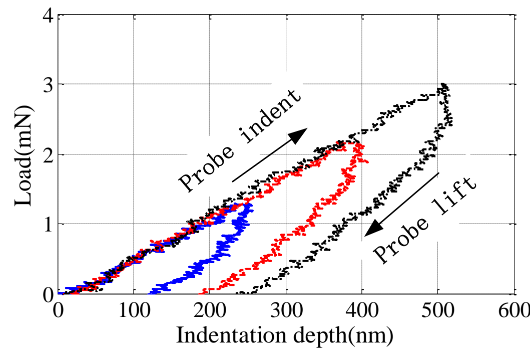

(b) The load versus the indentation depth

Fig. 6 The indentation tests of silicon

3.3 The effect of machining parameters on the micro/nano scratching

3.3.1 Scratching direction

Due to the symmetric structure of the Berkovich probe, the scratching in the d3 and d4 directions has the same characteristics, so they are combined together. Based on the four directions defined in Fig. 3, the relationships between the normal load and scratching depth are analyzed and shown in Fig. 7. It is obvious that the scratching depth increases as the normal load increases in all four directions. With the same normal load, the scratching depth in the d2 direction is the largest, while in the d1 direction is the smallest.

Generally, the normal load is considered as the product of the sample yield stress and the horizontal projected area of the tip-sample interface [14-16, 28]. Based on the horizontal projected area in Fig. 3(b), for the same normal load, the scratching depth in the d1, d3 and d4 directions should be half of it in the d2 direction, but the experimental results are not agree well in Fig. 7. The possible reason is that in the scratching direction d2, the cutting tool is a pyramidal face rather than a blade, which leads to the material stack in front of the probe tip, as a result, the tip-sample interface is increased greatly, thus resulting in the reduction of scratching depth, this phenomenon

has been found in the scratching simulation [29]. The scratching depth in the d1 direction is smaller than those in the d3/d4 directions, this may be caused by the assembly error of the probe. As shown in Fig. 8, assuming the probe is assembled with a tilted angle θ towards the d1 direction. On the one hand, it directly leads to the increase of the tip-sample interface due to the probe tilt. On the other hand, the attack angle δ is reduced with a tilted angle, which is against to remove the material, further resulting in the increase of tip-sample interface. All these reasons will reduce the scratching depth.

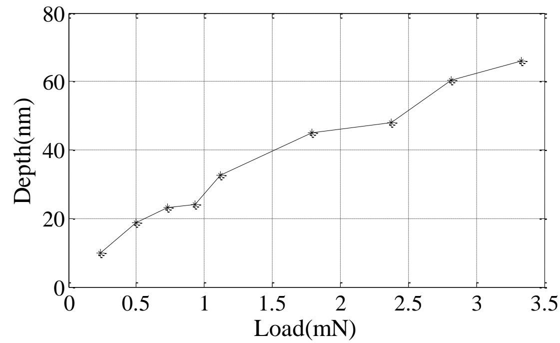

(a) d1 direction

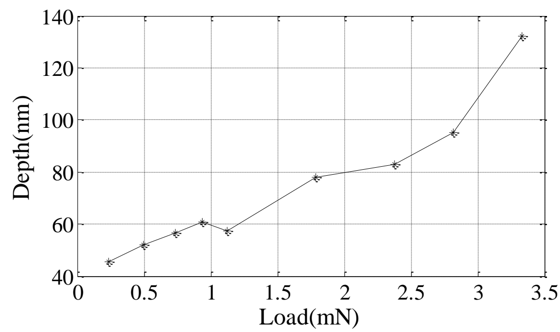

(b) d2 direction

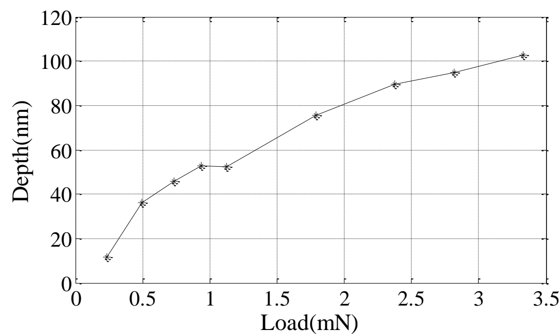

(c) d3/d4 direction

Fig. 7 The relationship between the normal load and scratching depth

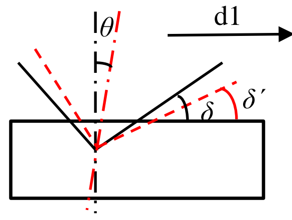

Fig. 8 The tilt of the probe tip

3.3.2 Scratching cycles

In the exploration of multi scratching, the scratching direction is the d3/d4 direction, the normal load is 1.5 mN and the scratching speed is 5 μm/s, the scratching numbers of scratching cycles are set as 1, 2, 5 and 10, respectively. According to the experimental results as shown in Fig. 9, the scratching depth is increased gradually from 70 nm in 1 scratching cycle to 170 nm in 10 cycles, the same trend as other scholars' reports [7, 30]. Besides the increase of the scratching depth, it can also be seen that the groove wall, especially the right side, in 1 scratching cycle is coarser than the multi scratching. In order to show this phenomenon better, a section of groove bottom is shown in Fig. 10, which indicates the groove undulation in 1 scratching cycle is almost twice to it in 10 scratching cycles. It is because with the increase of the scratching cycles, the groove wall and bottom suffer repeated mechanical extrusion and friction, as a result, most of micro bulges and defects are removed or compensated, make the groove smoother.

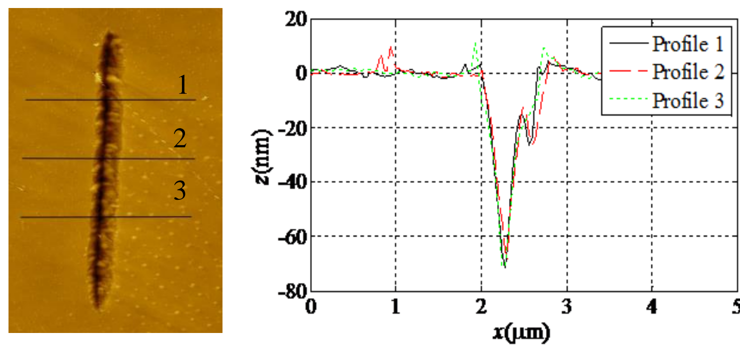

(a) 1 cycle

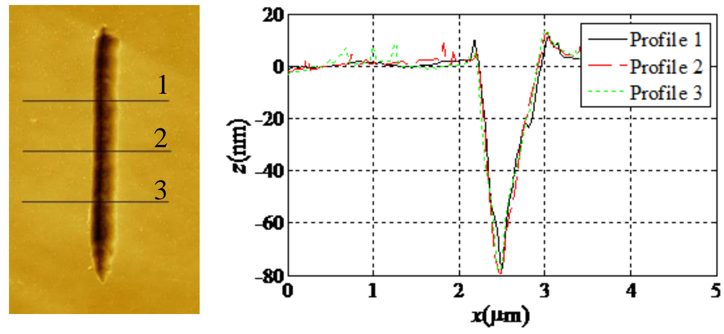

(b) 2 cycles

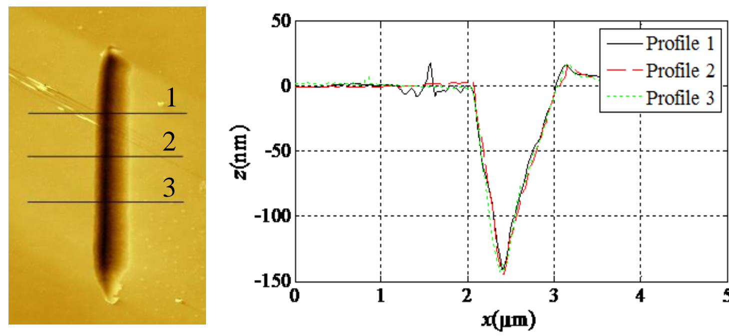

(c) 5 cycles

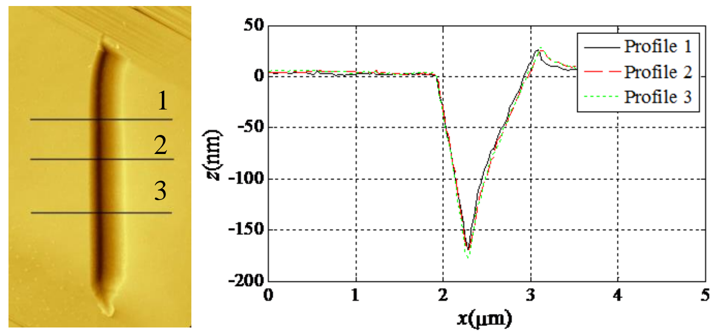

(d) 10 cycles

Fig. 9 Groove scratching with different numbers of scratching cycles

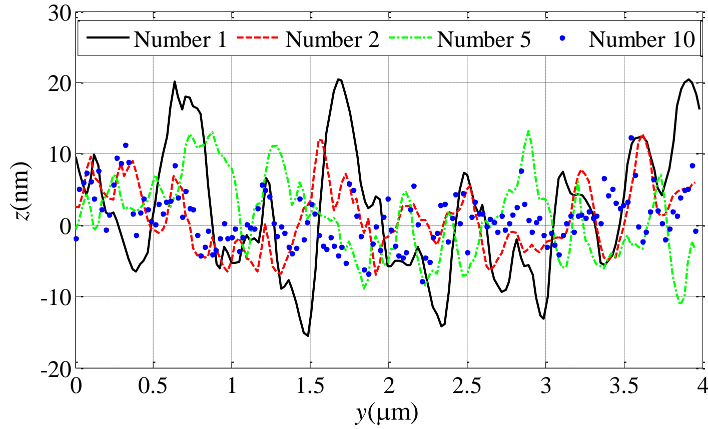

Fig. 10 The bottom of grooves with different scratching cycles

3.3.3 Scratching speed

In the scratching speed test, the normal load is kept constant, three scratching speeds of 2 μm/s, 5 μm/s, 10 μm/s are used for the experiments. The cross sections of the scratched grooves are shown in Fig. 11. The experiments show the average scratching depths with the three speeds are 48.0 nm, 49.8 nm and 49.8 nm respectively, the maximal difference is only 1.8 nm, indicating the scratching speed has little influence on the scratching depth.

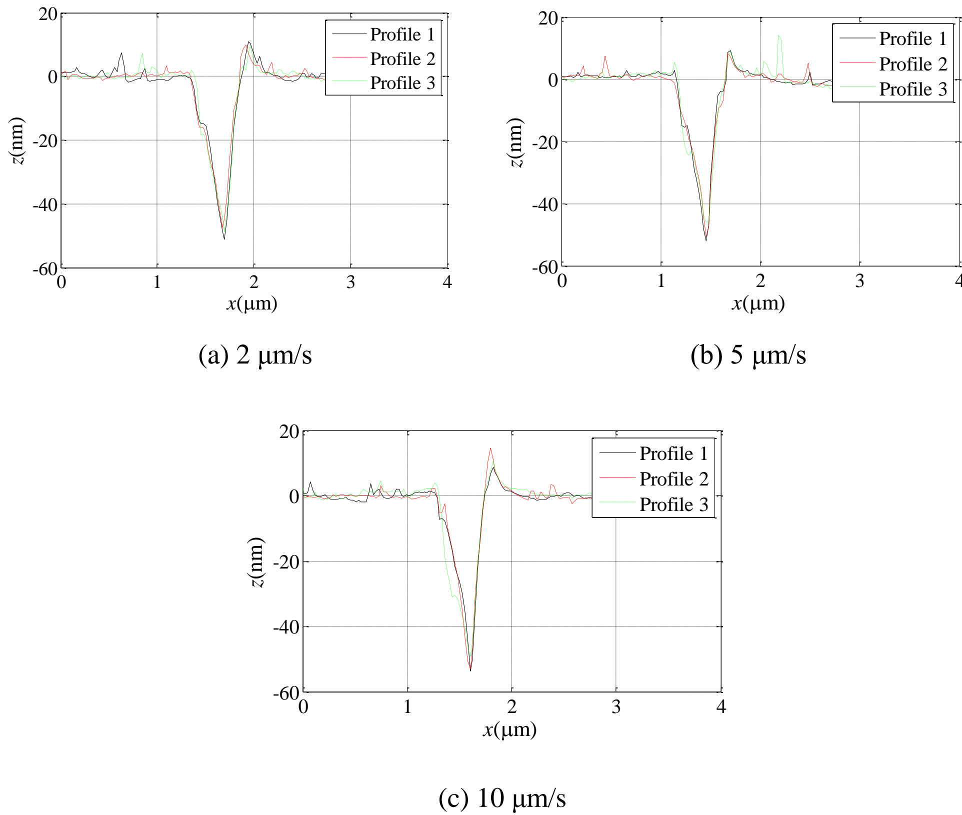

Fig. 11 Scratching depth with different scratching speed

3.3.4 Scratching feed

Only micro/nano grooves are scratched in the above experiments, a certain scratching feed is necessary to fabricate micro/nano structures, so the scratching feed is a very important parameter in the micro/nano machining. It has been verified that the scratching direction affects the scratching depth obviously, so in order to avoid this disturbance, the whole scratching in this section is the d3/d4 direction. Fig. 12 shows the probe trajectory. The probe is pressed into the sample during the scratching, when the micro/nano positioning stage is returned to initial position and generates feed movement, the probe is lifted up to avoid the additional scratching.

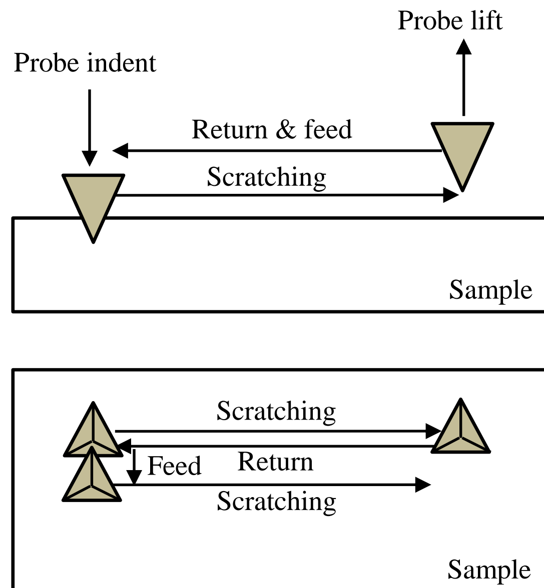

Fig. 12 The trajectory of the probe

Five feeds of 240 nm，160 nm，80 nm，60 nm，40 nm are selected to investigate the effect of feed on the micro/nano scratching. Other related parameters are as follows: normal load 0.75 mN, scratching speed 5 μm/s, scratching direction d3/d4. The scratching results are shown in Fig. 13. The groove is separated from each other in the larger feed of 240 nm and 160 nm, while in the smaller feed of 80 nm, 60 nm and 40 nm, a micro structure with certain depth is machined, the average depth is increased from 28.4 nm, 57.3 nm to 123.7 nm as the feed is reduced. This is because that the adjacent grooves are interlaced each other for a smaller feed, leading to the reduction of tip-sample interface area in subsequent scratching, as a result, the scratching depth is increased. The roughness (Ra) can be seen as an important parameter to define the machining quality, so the AFM images of the scratched micro structures are post-processed in Gwyddion software to obtain the surface roughness. In order to avoid the randomness, the roughness in three positions of the scratched surface are measured and then takes the average value. The results show

the roughness of the scratched surface with the feed 80 nm, 60 nm and 40 nm is 10.6 nm, 9.3 nm and 13.3 nm, respectively.

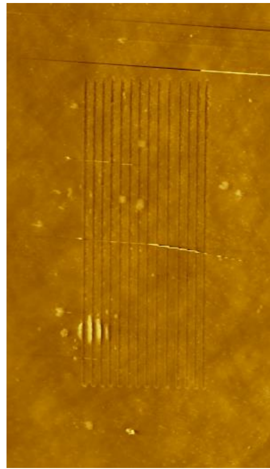

(a) feed of 240 nm

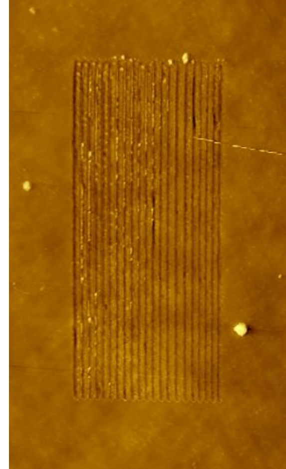

(b) feed of 160 nm

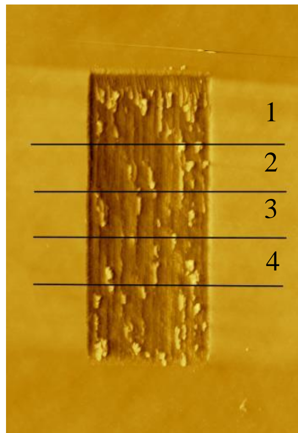

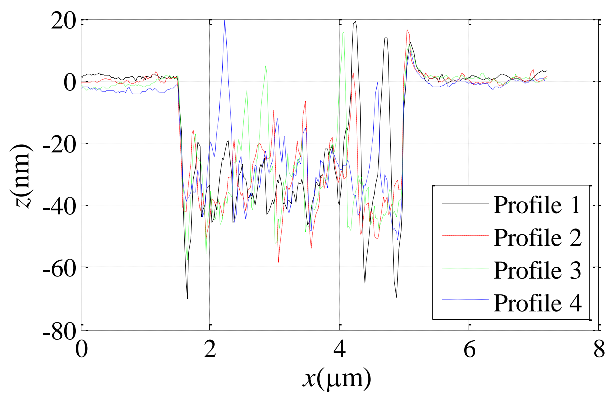

(c) feed of 80 nm

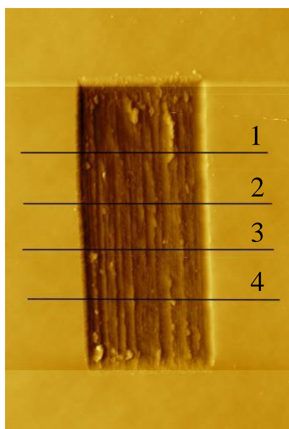

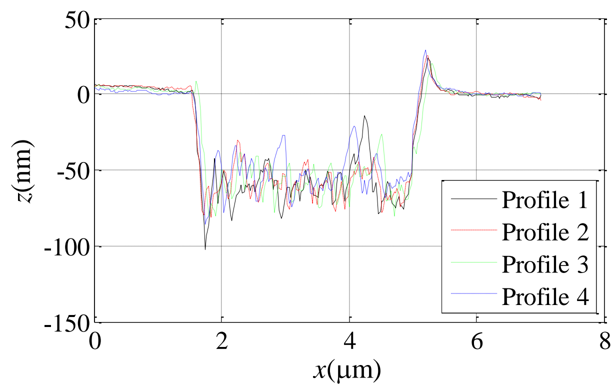

(d) feed of 60 nm

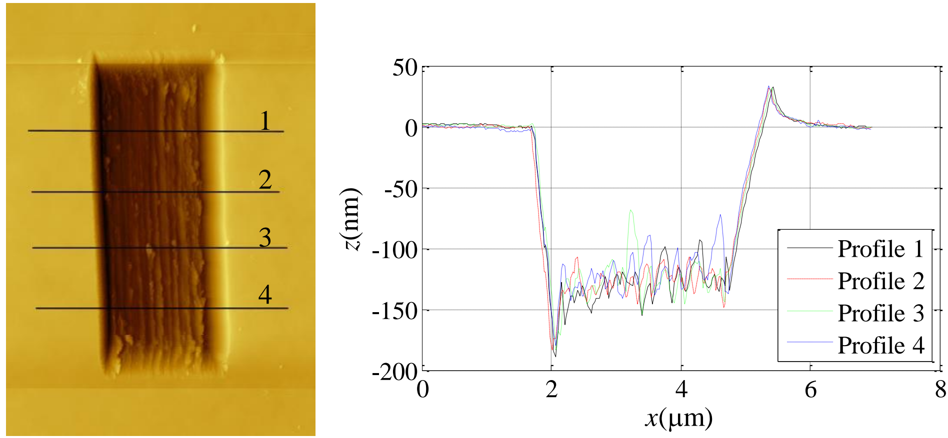

(e) feed of 40 nm

Fig. 13 The scratching results with different feed

It has been known that the normal load affects the scratching depth significantly in single scratching, so in the multi scratching with feed 60 nm, the effects of five different normal loads on scratching depth are explored. The relationship between the normal load and the scratching depth is shown in Fig. 14, indicating the scratching depth is increased with the increase of the normal load as a whole, but the increasing rate is slowed down in the larger scratching depth.

In the Geng's model [16], the normal force is the product of the horizontal projected area of the tip-sample interface and the yield stress, where the horizontal projected area is approximately a quadratic polynomial of the scratching depth, the yield stress is also related to the scratching depth, so a cubic polynomial is much closer to the model's equation power. Thus, in order to avoid the complicated theoretical modeling, a cubic polynomial is selected to fit the experimental normal load and scratching depth, the range of scratching depth is from 40 nm to 140 nm, the fitting function is optimized as Eq. (2), which can be used to predict the machining depth for the three dimensional micro/nano structure. It is noted that the fitted cubic polynomial is only applicable when the scratching depth is fallen in the depth range as it in the polynomial fitting process.

$$F_{\text{normal}} = 0.00000102h^3 - 0.00012947h^2 + 0.01610394h + 0.01792159 \tag{2}$$

where, F_{normal} and h is the normal load and scratching depth, respectively.

Another two scratching experiments have been conducted to further validate the effectiveness of the fitting function, and the results are marked as green circles in Fig. 14. Under the effect of normal force 0.73mN and 0.78mN, the experimental and predicted scratching depths are about 58 nm, 63 nm and 59.2 nm, 63.6 nm, respectively, the results agree well.

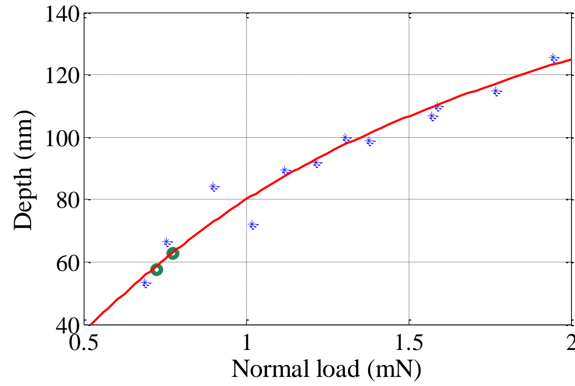

Fig. 14 The relationship between the normal load and scratching depth with feed 60 nm

3.4 The effect of sample material on the micro/nano scratching

Silicon is relatively hard, so another soft sample copper is scratched to compare the scratching property with silicon. The AFM image of the scratched grooves on copper is shown in Fig. 15. According to the profiles of the groove, it generates obvious ridge on the groove sides, and the chip is stacked in the end of the groove. While in the silicon scratching, as shown in Fig. 9(a), there are almost no ridge and residual chips on the groove sides. In conclusion, harder material is easier to be removed in the micro/nano scratching, which is favorable in three dimensional micro/nano structure machining, but excessive hard sample material usually accelerate the wear of the probe tip.

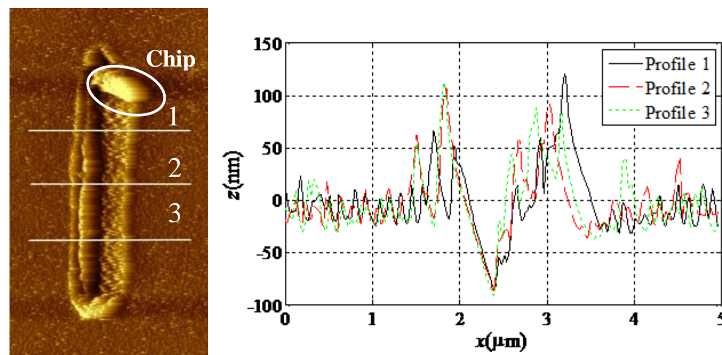

Fig. 15 The scratching of copper

4. Three dimensional micro/nano machining

Based on the above experimental results, some additional three dimensional micro/nano structures are fabricated on silicon substrate by controlling the normal force. The following machining parameters are adopted: scratching direction d3/d4, scratching speed 5 μm/s and feed 60 nm.

Fig. 16 shows the normal force used for the fabrication of a stair micro/nano structure and the

corresponding experimental result. The average scratching depth in right stair is about 10nm smaller than the left one, the possible reason is that the sample is not ideally horizontally positioned. The surface roughness in three stairs from left to right are 13.2, 19.5 and 10.7nm, respectively, indicating that larger scratching depth makes the scratched surface coarser. Similarly, a sinusoidal micro structure is fabricated with a magnitude of normal force 0.6 mN, which is shown in Fig. 17. It is noted that in the machining of these two kinds of micro structures, the normal load is kept constant in every single scratching, but is controlled based on Eq. (1) in the feed direction.

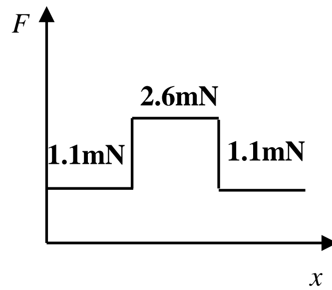

(a) the normal force

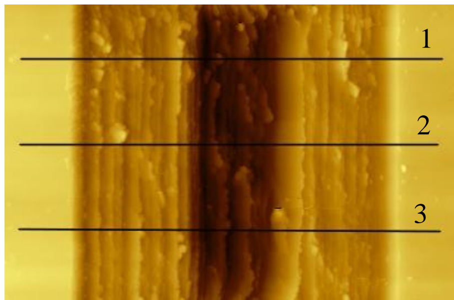

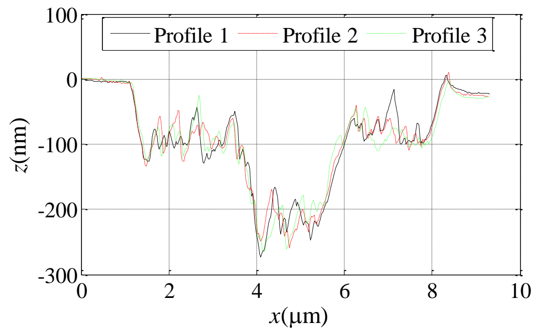

(b) the AFM image scratched micro stair (c) the profiles of the micro stair

Fig. 16 The micro/nano structure of stair

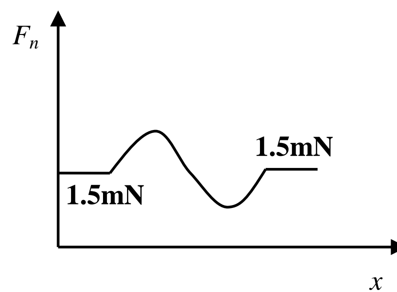

(a) the normal force

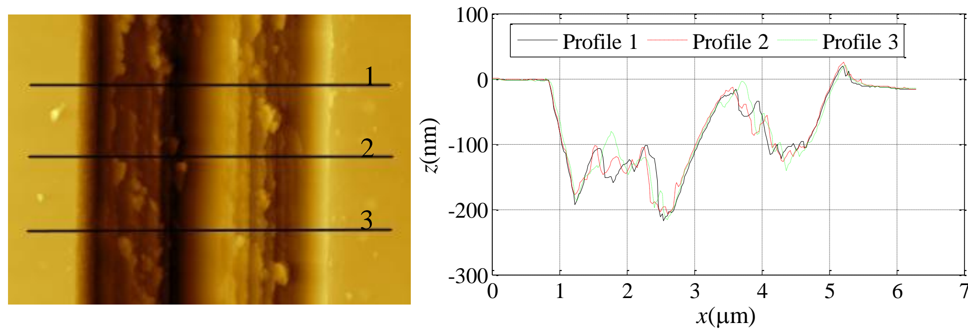

(b) the AFM image of sinusoidal micro structure (c) the profiles of sinusoidal micro structure

Fig. 17 The scratched sinusoidal micro structure

Furthermore, some complex three dimensional micro/nano structures are also fabricated. As shown in Figs. 18 and 19, a Chinese character '田' and an abbreviation of Tianjin University 'TJU' are fabricated, for these two micro structures, the normal force needs to be controlled in both single scratching and feed direction. The average scratched depth in two sides of micro structure '田' is about 130 nm, while the depth of four squares in the center is about only 90nm. This is may be caused by the tip geometry, the pyramidal surfaces of the tip form two slopes in both start and end of every single scratching, when the scratching length is small, the two slopes will occupy large volume of the scratched micro structure, thus make the scratching depth small. Same phenomena can be found on the top line of 'T' and 'J', the bottom line of 'U'.

A more complex micro structure, cartoon of Chinese panda, is further fabricated. The original picture and the AFM picture of the fabricated micro structure are shown in Fig. 20. Due to the complexity of the probe trajectory, the gray value of the original image is used to control the probe motion. According to the fabricated micro panda, the narrowest part of the panda is the mouth with channel width 0.3μm. It is worth to indicate a sharper probe tip is helpful to fabricate a narrower channel.

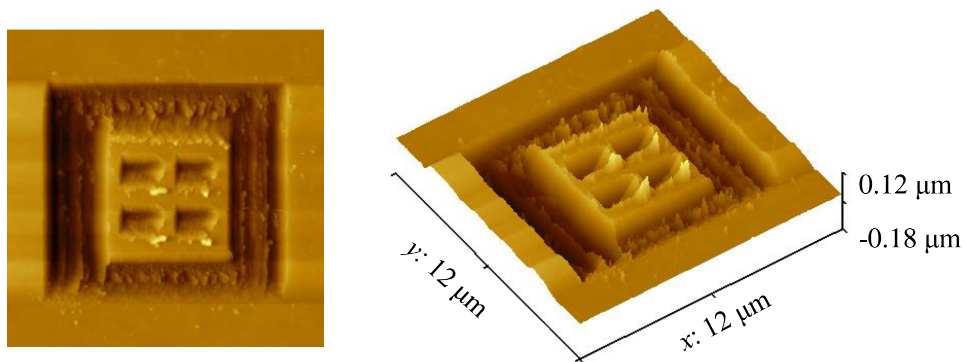

Fig. 18 Chinese character "田"

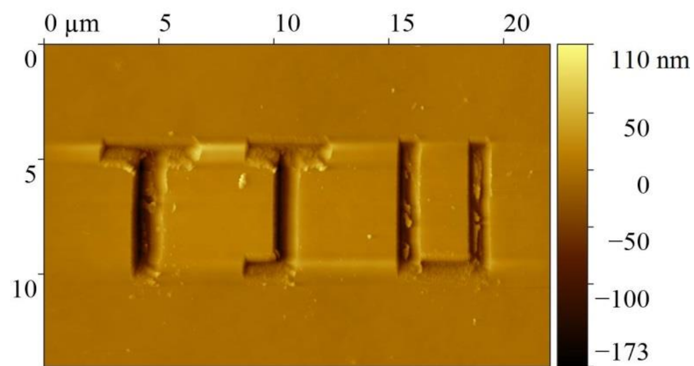

Fig. 19 Abbreviation of Tianjin University - TJU

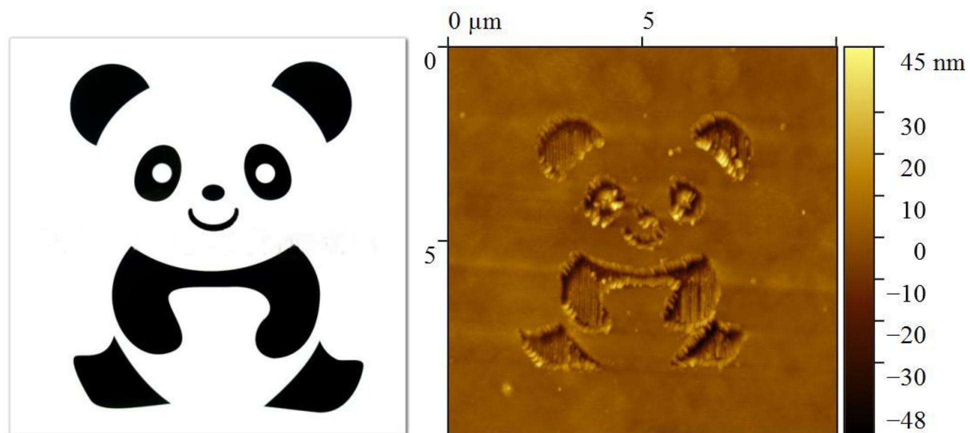

Fig. 20 Three dimensional micro structure of Chinese panda

5. Conclusion

In the micro/nano machining, the machining parameters include scratching direction, normal load, scratching cycles, scratching speed and feed amount. According to the experimental results,

the scratching depth in the d2, d3/d4 and d1 directions is successively reduced, but it is affected more obvious by the normal load. Multi scratching can also increase the scratching depth, and the groove become smoother as the number of scratching cycle number increases. The scratching depth difference is only 1.8 nm in three scratching speed, implying the scratching speed has little influence on the scratching depth. Compared with the scratching on silicon, the copper is easier to generate ridges in the groove scratching, indicating that the harder material is easier to be removed. In the scratching with feed, the micro structure was machined when the feed is smaller than 0.08μm, and the machined depth increases as the feed reduces.

Based on the analysis of machining parameters on scratching process, the scratching direction d3/d4, scratching speed 5μm/s and feed 60 nm are selected for the micro structure machining. Through the motion control of probe, the micro structures including stair, sine, Chinese character '田', 'TJU' and Chinese panda are machined on the silicon base, which demonstrate the feasibility of the selected machining parameters and the micro machining ability of the developed three dimensional micro/nano machining system.

There are still some drawbacks in the current machining system and the control method. In future work, a sharper probe tip will replace the Berkovich probe to reduce the channel width, and an automatic controlled horizontal leveling mechanism for the sample need to be designed. A feedback controller can be used to improve the controlling precision of the probe.

Acknowledgements

This research is supported by National Natural Science Foundation of China (Nos. 51675371, 51675367, 51675376, 51405333, 51420105007) and EU H2020 FabSurfWAR (No. 644971).

References

[1] W. Wu, D. Dey, O. Memis, Fabrication of large area periodic nanostructures using nanosphere photolithography, Nanoscale research letters, 3(10) 2008, pp. 351-354.

[2] E. Beeker, W. Ehrfeld, P. Hagmann, et al., Fabrication of microstructures with high aspect ratios and great structural heights by synchrotron radiation lithography, galvanoforming, and Plastic moulding (liga process). Microelectronic Engineering, 4(l) (1986), pp. 35-56.

[3] C. Kim, S. Ahn, D. Jang, Review: Developments in micro/nanoscale fabrication by focused ion beams. Vacuum, 86 (2012), pp. 1014-1035.

[4] N. Kooy, K. Mohamed, L. Pin, et al., A review of roll-to-roll nanoimprint lithography, Nanoscale research letters, 9 (2014), p. 320.

[5] A. Malshe, K. Rajurkar, K. Virwani, et al. Tip-based nanomanufacturing by electrical, chemical, mechanical and thermal processes. Cirp Annals - Manufacturing Technology, 59 (2010), pp. 628-651.

[6] Y. Yan, Y. Geng, Z. Hu, Recent advances in AFM tip-based nanomechanical machining, International Journal of Machine Tools & Manufacture, 99 (2015), pp. 1–18.

[7] T. Fang, C. Weng, J. Chang, Machining characterization of the nano-lithography process using atomic force microscopy. Nanotechnology, 11(3) (2000), pp. 181–187.

[8] T. Fang, W. Chang, effects of AFM-based nanomachining process on aluminum surface. Journal of Physics and Chemistry of Solids, 64(6) (2003), pp. 913–918.

[9] Y. Yan, T, Sun, et al, Investigation on AFM-based micro/nano-CNC machining system. International Journal of Machine Tools & Manufacture, 47 (2007), pp. 1651–1659.

[10] Y. T. Mao, K. C. Kuo, C. E. Tseng, et al., Research on three dimensional machining effects using atomic force microscope, Review of scientific instruments, 80 (2009), p. 065105.

[11] Y. Geng, Y. Yan, X. Zhao, Fabrication of millimeter scale nanochannels using the AFM tip-based nanomachining method, Applied Surface Science, 266 (2013), pp. 386-394.

[12] P. Zhang, H. Zhao, C. Shi, et al., Influence of double-tip scratch and single-tip scratch on nano-scratching process via molecular dynamics simulation, Applied Surface Science, 280 (2013), pp. 751–756.

[13] K. Bourne, S. G. Kapoor, R. E. DeVor, Study of a high performance AFM probe-based microscribing process, Journal of Manufacturing Science and Engineering, 132(3) (2010), p. 030906.

[14] Z. Wang, N. Jiao, S. Tung, et al., Atomic force microscopy-based repeated machining theory for nanochannels on silicon oxide surfaces, Applied Surface Science, 257 (2011), pp. 3627-3631.

[15] Z. Wang, N. Jiao, S. Tung, et al., Material removal model for AFM-based nanochannel fabrication, Wear, 278 (2012), pp. 71-76.

[16] Y. Geng, Y. Yan, Y. Xing, Modelling and experimental study of machined depth in AFM-based milling of nanochannels, International Journal of Machine Tools & Manufacture, 73 (2013), pp. 87–96.

[17] Z. Lin, Y. Hsu, A study of estimating cutting depth for multi-pass nanoscale cutting by using atomic force microscopy, Wear, 258 (2012), pp. 4513-1522.

[18] J. Lee, W. Jin, D. Kim, Application of single asperity abrasion process for surface micro-machining. Wear, 251 (2001), pp. 1133–1143.

[19] J. Park, K. Kwon, J. Bang, et al., Development of a precision indentation and scratching system with a tool force and displacement control module. Review of Scientific Instruments, 78 (2007), p. 045102.

[20] W. Jeong, C. Soo, C. Hyun, Portable nano probe for micro/nano mechanical scratching and measuring. Trans. Nonferrous Met. Soc. China, 21(1) (2011), pp. S205−S209.

[21] B. Gozen, O. Ozdoganlar, Design and evaluation of a mechanical nanomanufacturing system for nanomilling, Precision Engineering, 36(1) (2012), pp. 19-30.

[22] X. Tang, I. Chen, Q. Li, Design and nonlinear modeling of a large-displacement XYZ flexure parallel mechanism mechanism with decoupled kinematic structure, Review of Scientific Instruments, 77(11) (2006), p. 115101.

[23] J. Pinskier, B. Shirinzadeh, L. Clark, et al., Design, development and analysis of a haptic enabled modular flexure mechanism, Mechatronics, 40 (2016), pp. 156-166.

[24] U. Bhagat, B. Shirinzadeh, L. Clark, et al., Design and analysis of a novel flexure-based 3-DOF mechanism, Mechanism and Machine Theory, 74 (2014), pp. 173-187.

[25] Y. Yong, B. Bhikkaji, S. Moheimani, Design, Modeling, and FPAA-Based Control of a High-Speed Atomic Force Microscope Nanopositioner, IEEE/ASME Transactions on Mechatronics, 18(3) (2013), pp. 1060-1071.

[26] Z. Guo, Y. Tian, J. Tian, et al., Probecopper system design for three dimensional micro/nano scratching machine, Microsystem Technologies, (2016), doi: 10.1007/s00542-016-3115-9.

[27] Z. Guo, Y. Tian, C. Liu, et al., Design and control methodology of a 3-DOF flexure-based mechanism for micro/nano positioning, Robotics and Computer Integrated Manufacturing, 32 (2015), pp. 93-105.

[28] D. Tabor, The Hardness of Metals, Oxford University Press, Oxford, 1951

[29] Z. Guo, Y. Tian, X. Liu, et al., Modeling and simulation of the probe tip based nanochannel scratching, Precision Engineering, (2017), doi: 10.1016/j.precisioneng.2017.02.002.

[30] Y. Geng, Y. Yan, B. Yu, et al., Depth prediction model of nano-grooves fabricated by AFM-based multi-passes scratching method, Applied Surface Science, 313 (2014), pp. 615–623.